Research and Development of Automated Eddy Current Testing for Composite Overwrapped Pressure Vessels

Kyle L. Carver

JSC-White Sands Test Facility

Major: Mechanical Engineering

NMSG Summer Session

Date: 27 Aug 12

Research and Development of Automated Eddy Current Testing for Composite Overwrapped Pressure Vessels

Kyle L. Carver[1], Regor L. Saulsberry[2], Charles T. Nichols[2], Paul R. Spencer[3], and Ralph E. Lucero[4]
NASA-JSC White Sands Test Facility, 12600 NASA Rd., Las Cruces, NM, 88012

Eddy current testing (ET) was used to scan bare metallic liners used in the fabrication of composite overwrapped pressure vessels (COPVs) for flaws which could result in premature failure of the vessel. The main goal of the project was to make improvements in the areas of scan signal to noise ratio, sensitivity of flaw detection, and estimation of flaw dimensions. Scan settings were optimized resulting in an increased signal to noise ratio. Previously undiscovered flaw indications were observed and investigated. Threshold criteria were determined for the system software's flaw report and estimation of flaw dimensions were brought to an acceptable level of accuracy. Computer algorithms were written to import data for filtering and a numerical derivative filtering algorithm was evaluated.

Nomenclature

COPV	=	composite overwrapped pressure vessel
ET	=	eddy current testing
ID	=	inner diameter
NDE	=	nondestructive evaluation
OD	=	outer diameter
SHM	=	structural health monitoring
S/N	=	serial number
TA	=	test article

I. Introduction

Composite overwrapped pressure vessels (COPVs) have become crucial components in aerospace systems. NASA systems incorporating COPVs include the Space Shuttle, International Space Station, Space Launch System, and Orion Crew Capsule. Many satellite systems also make use of COPVs. A possible weight reduction of up to 50 percent, when compared to a traditional metallic pressure vessel, gives great motivation to push forward in the understanding and development of COPVs.

Upon production a COPV metal liner can possess minute flaws that can be overlooked by visual inspection and liquid penetrant testing. If these flaws are not identified they have the potential to cause a leak before burst (LBB) failure of the COPV. The fact that liquid penetrant testing is also time consuming and can miss smaller flaws adds to the need for a more efficient and sensitive nondestructive evaluation (NDE) method to inspect these liners before the composite overwrap is applied. Identification of liner flaws prior to overwrap application is crucial due to subsequent flaw growth that can occur during autofrettage and subsequent pressure cycling during service. Autofrettage consists of pressurizing the vessel slightly beyond the liner's plastic yield point, leaving the liner under a state of residual compressive stress that is imposed by the composite overwrap. While this one-time process improves the consistency of the final product, there is the risk of causing fatigue growth of liner flaws. Once the overwrap is applied, it poses an inspection problem since the outer liner surface is no longer accessible, precluding the use of traditional methods such as liquid penetrant and magnetic particle testing. Also, sensitivity is reduced since any external NDE of the liner must be performed through the composite overwrap.

[1] NMSG Intern, Department of Mechanical & Aerospace Engineering, New Mexico State University, Las Cruces, New Mexico, 88003.
[2] Project Manager, NASA-JSC White Sands Test Facility, Laboratories Department, MS 200LD, Las Cruces, New Mexico 88004.
[3] Metallurgical Engineer, NASA-JSC White Sands Test Facility, Laboratories Department, MS 201LD, Las Cruces, New Mexico 88004.
[4] Mechanical Engineer, NASA-JSC White Sands Test Facility, Laboratories Department, MS 200LD, Las Cruces, New Mexico 88004.

These unique problems call for a NDE method that are can be applied prior to wrapping of the bare liner, can be used to inspect the inside surface of the liner after wrapping, or that has sufficient sensitivity to interrogate the liner through the overwrap. Eddy current testing (ET) is a NDE technique that solves the above problems and is being investigated as a reliable way to inspect COPV liners.

II. Background

A. Eddy Current Testing

ET has been extensively used to inspect specimens such as solid bars, tubes, rivets, welds, and aircraft components for cracks, corrosion, pitting, and other types of metallurgical flaws. In general, ET scanning consists of a probe coil through which a current is passed. This coil is brought in contact with or in close proximity to a test specimen. The magnetic field generated by the coil creates rotating currents in the specimen called eddy currents. When the probe is moved over a discontinuity there is a change in the eddy currents. These changes can be detected using a secondary "receiver" coil or by observing changes in the primary "excitation" coil. This limits the test specimens to conductive or semi-conductive materials. Perhaps the most significant advantage of the ET method is its inherent sensitivity to many material variables and the resultant versatility; however, the problems caused by this sensitivity also beget its greatest limitation. Thickness, surface finish, electrical conductivity, and magnetic permeability are several variables that can affect scan signal [1, 2, 3].

B. Multipurpose Vessel Scanner

Recently the NASA White Sands Test Facility (WSTF) Materials and Components Laboratories Office has integrated an external eddy current scanner into their laser profilometry system. This system is capable of automatically scanning cylindrical metal liners with lengths up to 51 cm (20 in.) and diameters of roughly 17 cm (6.5 in.). The system operates by rotating the test article (TA) while the probe travels along the surface of the TA. This innovative system can rapidly scan liner surfaces with minimal operator supervision. In general, scans range from 5 to 40 min depending on the scan area and scan resolution. The system consists of a Uniwest US-454A EddyView scanning unit, and a LTC LP-4000 processer paired with a LTC Motor Control Unit (Figure 1). A variety of probes were used during this study (Table 1). An innovative sensor manipulation and delivery system has been designed to allow internal inspection, which will be particularly useful for inspecting wrapped COPVs.

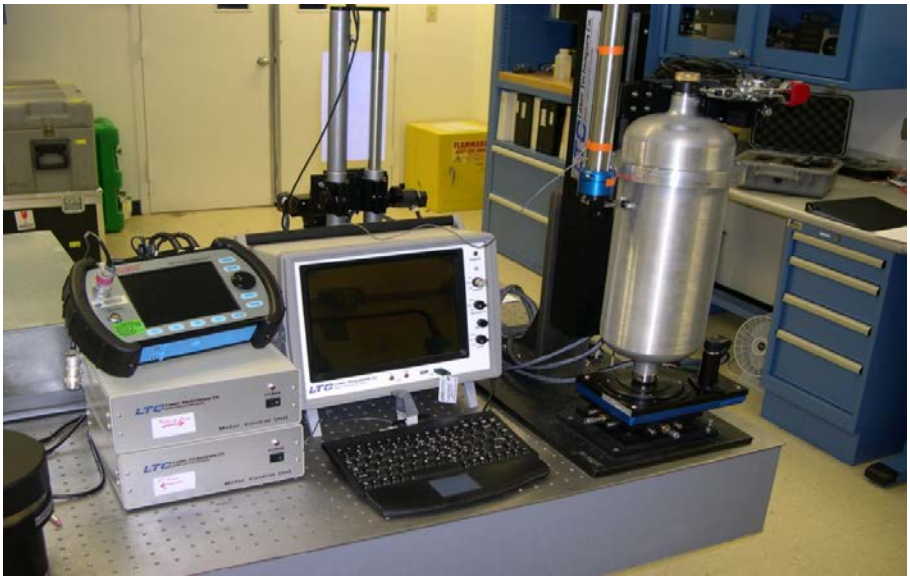

Figure 1. Uniwest US-454A EddyView (top left), LTC Motor Control Unit (lower left), LTC LP-4000 (middle), Probe and Test Article (right)

Table 1. Probes used at WSTF for scanning COPV liners.

Probe ID	US-2298	US-2755	US-2832	ENGDEV-1	ENGDEV-2
Application	Linear discontinuities on the scanning surface	Liner ID w/o overwrap	Linear discontinuities on the scanning surface	Liner OD w/ overwrap	Liner OD w/ overwrap
Frequency Range	1-3 MHz	0.5-35 kHz	1-10 MHz	0.2-3 kHz	0.2-3 kHz
Operating Mode	abs/ref	abs/ref	diff/ref	abs/ref	abs/ref
Coil Location	juxtaposition	coaxial	juxtaposition	juxtaposition	juxtaposition
Preferred Orientation	±30°	None	±35-40°	±30°	±30°
Shielding	Ferrite	Ferrite	None	None	Ferrite
Air Core	No	No	No	Yes	No

III. Experimental

A. General Scanning Process

External scans on bare liners were conducted by installing the selected probe and TA into the system. The probe coordinates were then zeroed at a predetermined location on the surface of the test article. In general, zero in the rotary direction corresponds with a known witness mark ("S" in the TA's S/N was used in this study) while the zero in the linear direction is given by the upper edge of the cylindrical shell of the vessel where the head and shell intersect, often referred to as the "shoulder". The probe was then moved to the area to be scanned. Once the scan and probe settings were entered into the system, the probe was moved across the surface of the TA as the TA was rotated at a specified scan speed, typically at 30 rpm, as data was recorded. For every rotation the probe completed, a step of the magnitude of the linear resolution was taken in the linear direction until the scan interval was completed.

B. System Verification

WSTF operators' previous settings (table 2, column 1) and scan data were used as a baseline for the scan results presented in this paper. Scans were completed with the baseline settings to verify system reproducibility. During testing, the US-2298 probe was deemed unfit for use due to mechanical failure caused by repeated stress on the probe wiring. The faulty wiring would produce massive spikes in signal at random. This limited scans to the remaining four probes: US-2755, US-2832, ENGDEV-1, and ENGDEV-2.

Table 2. Settings for the US-454A EddyView partnered with the US-2832.

Baseline Settings	*Optimized Settings*
Frequency = 2.00 MHz	Frequency = 2.70 MHz
Gain = 60 dB	Gain = 60 dB
Rotational = 105°	Rotational = Varies
Probe Drive = High	Probe Drive = High
Low pass filter = 370 Hz	Low pass filter = 400 Hz
High pass filter = 150 Hz	High pass filter = 90 Hz
X sensitivity = 1 V/div	X sensitivity = 2 V/div
Y sensitivity = 1 V/div	Y sensitivity = 2 V/div

C. Liner and Liner Scans

Throughout the main course of the project the US-2832 probe was used to scan bare 6061-T6 aluminum liners S/N 18097 and S/N 18076, manufactured by Samtech Engineering and Composites (Uttar Pradesh, India). The thickness of each liner scanned varied from 2.032 mm (0.080 in.) to 3.175 mm (0.125 in.) over the range of the cylindrical portion. These liners possessed fatigue fractures that were intentionally initiated and propagated via pressure cycling (pressure unknown). Liner S/N 18097 had undergone eight thousand pressure cycles leaving the liner with four areas containing a total of six confirmed linear discontinuities along with two unreported linear discontinuities (Table 3). Liner 18076 did not have a reported number of pressure cycles and possessed three

confirmed linear discontinuities. A well-tested ET system at NASA Langley Research Center (LaRC) was used to determine the actual flaw dimensions (system model number and probe S/N unknown).

Table 3. Flaw descriptions for liner S/N 18097**.**

Location (deg., in.)	*Number of Cracks*	*Length (2c) (in.)*	*Depth (a) (in.)*	*Aspect Ratio (a/2c)*
55, 7.80	2	0.1125, unreported	0.0048, unreported	0.043, unreported
70, 9.30	1	unreported	unreported	unreported
235, 11.80	3	0.0750 ,0.0900, 0.0675	0.0045, 0.0052, 0.0051	0.060, 0.058, 0.076
323, 12.60	1	0.2250	0.0048	0.021
334, 3.08	1	0.0360	0.0055	0.15

To simulate a scan for the purpose of adjusting scan settings, the installed probe was placed over a known discontinuity and the test article was rotated at the specified scan speed. As the probe passed over the discontinuity, an indication was produced and would then be displayed on the US-454A EddyView. To optimize settings, the signal was observed as each setting was varied in the following order. First, a frequency was input followed by an adjustment of the rotational setting to control noise. Then the low and high pass filters were varied to allow the greatest signal amplitude while minimizing noise.

D. Data Analysis

The LaserViewer 2010 (Laser Techniques Co., Redmond, WA) flaw reports consist of signal peaks, discontinuity locations and discontinuity dimension estimations. The criteria for a discontinuity to be flagged are a minimum number of pixels in the X and Y direction with specified minimum signal amplitude. The height and width of each pixel corresponded with the X and Y resolution of the scan. Settings were varied and results were compared to the actual flaw dimensions.

Code was written using MATLAB (MathWorks, Natick, MA) to import the data to apply various derivative style filtering algorithms. From there, a three-point estimation method, Equation (1), was used to calculate the derivative

$$f'(x) = \frac{f(x+h) - f(x-h)}{2h} \tag{1}$$

which was then plotted and compared to the original data. This process was repeated to obtain second derivative plots which were compared with the first derivative and original plots in hopes of obtaining a higher signal to noise ratio.

IV. Results

A. Scan Results

Following the process described above, settings were optimized (Table 2, column 2) to improve the scan sensitivity. Results were improvements in scan clarity allowing for easier visual flagging of discontinuities. Filtering the data using data processors built into the software was helpful in reducing noise levels. The number of visual false flaw identifications was significantly reduced. However, the changes in settings also resulted in the reduction of signal amplitude for the smallest flaw on the S/N 18097 liner. The left image of Fig. 2 shows a scan of the one of the smallest discontinuities (Table 3, first line) obtained with the optimized settings while the right image shows a close-up view of the indications. The uppermost indication represents the smallest discontinuity on the S/N 18097 liner and bottom indication is a distinct, easily detectable flaw. Figure 3 shows two rows of data taken from US-2832 scans at 7.83 in. on the S/N 18097 liner. The signal indication at the 50 deg. mark represents a known flaw while the remaining signal indications correlate with no known flaws (false positives).

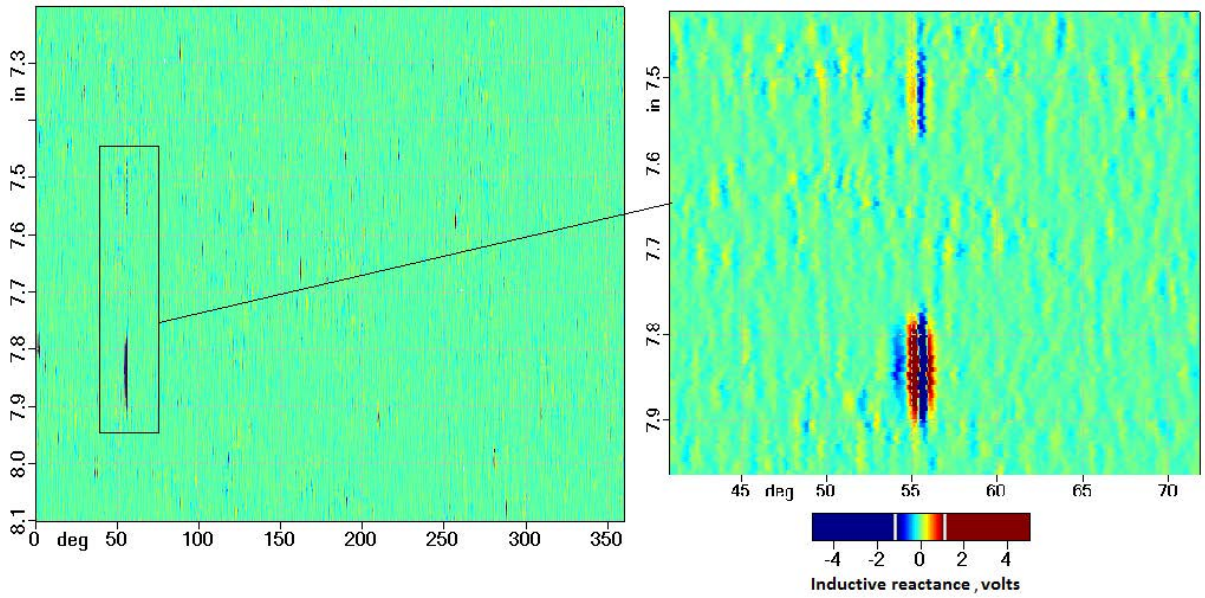

Figure 2. US-2832 Scan 19 of liner S/N 18097. Scan Overview (left) and Flaw Zoom (right).

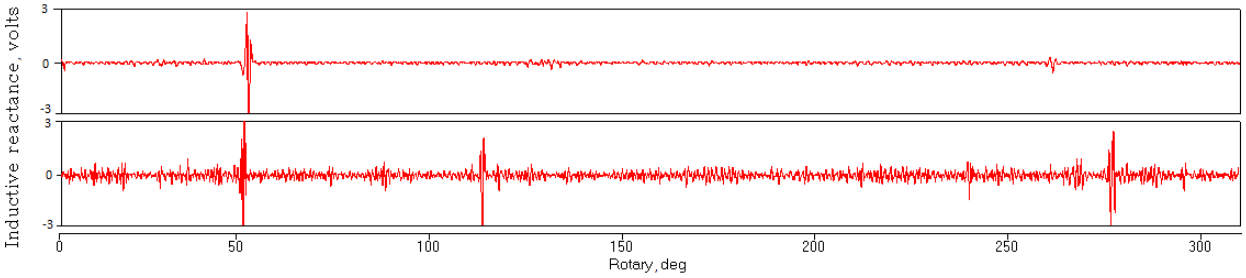

Figure 3. Optimized (top) vs. baseline (bottom) scan signals at 7.83 in. on liner S/N 18097 taken from US-2832 scans 3 and 19.

B. Flaw Report

Minimum detectable flaw criterion for scans of 0.05 to 0.13 mm (0.002 to 0.005 in.) resolution consisted of minimum amplitude of 1 volt, 10 pixels in the X direction, and 30 pixels in the Y direction. This translated to a cluster width of 0.51 mm (0.020 in.) and length of approximately 1.5 mm (0.060 in.). These dimensions were used as a baseline cluster size for all scan resolutions. Flaw report results were able to estimate crack lengths within a tolerance of ± 0.15 mm (0.006 in.) of the actual crack dimensions. However, this accuracy only appeared in high resolution scans (Table 4). Low resolution survey scans resolutions of approximately 0.5 mm (0.02 in.) and above, grossly overestimated crack lengths but still correctly flagged the known flaws (Table 3, line 3).

Table 4. Flaw report data for discontinuities in liner 18097 located at 235.26°, 11.80”

Scan Name	*Scan Linear Resolution (in.)*	*Flaw ID*	*Reported Length (in.)*	*Actual Length (in.)*	*Error (in.)*
US-2832 Scan 21	0.002	Cl 1	0.094	0.090	+0.004
		Cl 2	0.080	0.075	+0.005
		Cl 3	0.062	0.068	-0.006
US-2832 Scan 17	0.025	Cl 1	0.125	0.090	+0.035
		Cl 2	0.125	0.075	+0.050
		Cl 3	0.125	0.068	+0.057

C. Previously Undiscovered Indications

Several scans of the S/N 18097 liner produced indications with signal amplitude of approximately 0.50 volts. Originally these indications were thought to be noise, however the signals occur at consistent locations and amplitudes throughout scans obtained with both the US-2832 and US-2298 probes. While these indications were similar in both amplitude and size to several small confirmed flaws, they were oriented in the opposite sign voltages of the confirmed flaws as shown in Fig. 4. It was speculated that the indications may be subsurface flaws, for

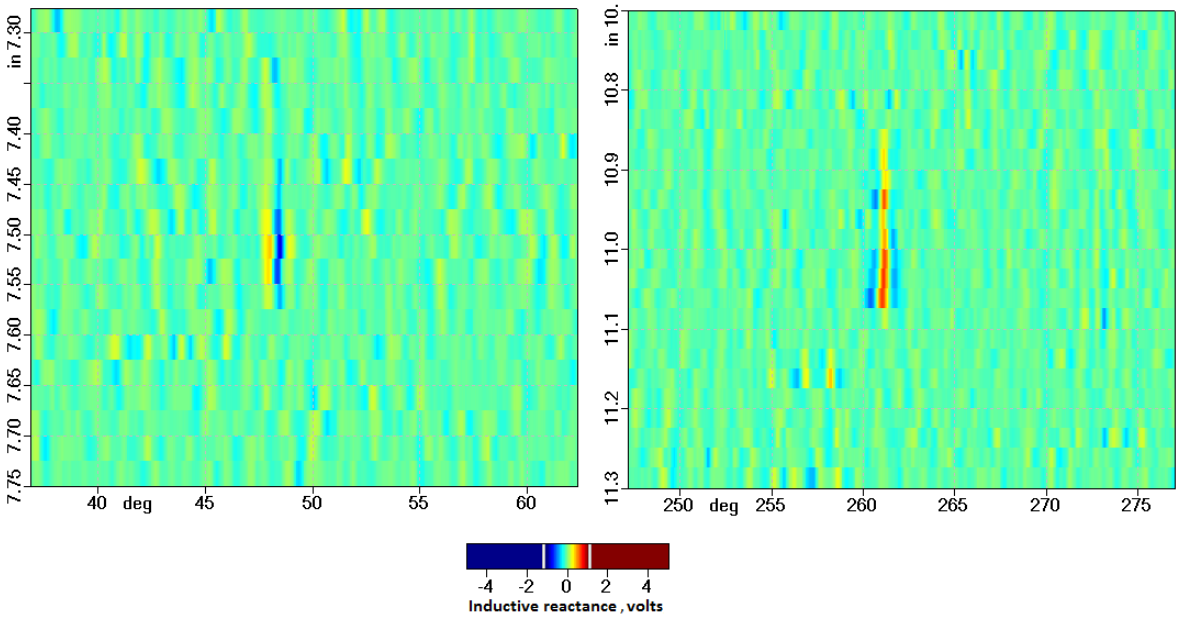

Figure 4. US-2832 Scan 19 of liner S/N 18097. Scan Overview (left) and Flaw Zoom (right).

example, inclusions; or flaws on the ID surface of the liner. To determine if it was possible to detect ID flaws, the depth of penetration for the given case was calculated (Equation (2)). The depth of penetration ( ) for a given test frequency (*f*) depends on the magnetic permeability ( ) and electrical conductivity ( ) of the test article: where , *f*, nd are in units of m, Hz, Hz/m, and 1/(ohm-m), respectively. One standard depth of penetration is defined as the depth at which the eddy current density is 37 percent of the material surface value. The eddy current density decreases rapidly as depth increases. The depths of penetration when scanning at 2.7 MHz and 2.0 MHz with the above probes are 0.061 mm (0.0024 in.) and 0.071 mm (0.0028 in.) respectively, less than the liner thickness. When scanning, a depth of penetration is selected so that it slightly surpasses the expected depth of the flaws. Therefore, when scanning with the US-2832 and US-2298 probes at 2.7 and 2.0 MHz, it was not possible to detect flaws on the ID of the liner, and the indication shown in Table 4 may be attributable to a subsurface flaw.

$$\delta = \frac{1}{\sqrt{\pi * f * \mu * \sigma}} \qquad (2)$$

D. Other Sensor Evaluations

Brief work with the ENGDEV-1 and ENGDEV-2 probes did not yield promising data for inspection surface scans as these probes were developed with low frequencies for deep penetration to scan through composite overwrap. An attempt was made to simulate the effects of scanning through an overwrap by placing several layers of tape between the probe face and the TA. This attempt was unsuccessful and work with the ENGDEV probes was halted due to the absence of an overwrapped TA with fully characterized liner discontinuities.

Work with the internal scanning attachment was hampered by problems in the attachment's original design. Adequate clearance for the wiring of the probe through the entrance port of the TA was not provided. Once the

alterations have been made to the internal scanning attachment, scans will be performed on the inside surfaces of the test articles.

V. Conclusion

Successful optimization of the US-2832 probe settings showed that it had the best sensitivity to the external flaws in the test specimens. Depth of penetration calculations clearly show that the weak signals of opposite sign orientation are not flaws on the ID of the vessel. The consistency of these indications, appearing in multiple scans obtained with two separate probes, implies that they are not noise but physical discontinuities. Further investigation of the suspected areas is planned.

The flaw report was successfully applied to newly obtained scans. The accuracy of flaw estimation was brought to within 5 percent of reported values when used with high resolution scans. The process of detecting flaws should be 1) obtain a low resolution survey scan to flag questionable areas, and 2) investigate questionable areas with a scan resolution of approximately 0.05 to 0.13 mm (0.002 to 0.005 in.) to accurately estimate flaw dimensions. A complication with the flaw report settings is that it involves setting a number of pixels in the X and Y directions for the minimum cluster criterion. This presents a problem as pixel dimensions vary with resolution settings. It is recommended that future versions of the software be modified so a unit of length, rather than a number of pixels, can be used to flag clusters of high amplitude signal.

The three-point estimation plots of the data's first and second derivatives showed no improvement in the signal to noise ratio. While the plot images seem to visually indicate improvements, the numerical ratios say otherwise. Although no significant improvements were made as a result of filtering the data, the groundwork was laid for future filtering to be applied as needed. The code written in MATLAB can be used to import the raw eddy current data so filters can be easily applied.

The two TAs examined over the course of the project provided good contrast. One produced very strong and distinct indications as opposed to the weak and indistinct indications of the other. However, two test articles provide a limited amount of data. The next step in this project, other than implementing the internal probe, is to obtain more test articles. With regards to the internal attachment, the US-2832 probe will be used in place or in tandem with the previously selected US-2298. It has been shown that this system can detect flaws with depths as shallow as 0.066 mm (0.0026 in.) and lengths as short as 0.91 mm (0.036 in.). These results easily satisfy NASA's minimum flaw size requirements for ET for bare COPV liners having a thickness greater than 1.3 mm (0.050 in.), Table 5 [4], of a minimum depth of 0.5 mm (0.020 in.) and minimum length of 2.5 mm (0.1 in.). Due to ET's ability to detect flaws smaller than the minimum detectable crack size for thicker (>1.3 mm (0.050 in.)) COPV liners, and inferred ability to detect flaws approaching the minimum detectable crack size for thinner (<1.3 mm (0.050 in.)) COPV liners, ET shows great promise for the NDE of COPV liners. With the COPV industry heading in the direction of thinner liners, detection of smaller flaws is critical. The progression of ET will allow for lighter and more reliable COPVs.

Table 5. Minimum initial crack size for partially through cracks [4]

NDE Method	Part Thickness t (in.)	Crack Depth a (in.)	Crack Length 2c (in.)
Eddy Current	t > 0.050	0.020	0.200
		0.050	0.100
Dye Penetrant	t > 0.075	0.025	0.250
		0.075	0.150
Magnetic Particle	t > 0.075	0.038	0.038
		0.075	0.250
Radiography	0.025 < t > 0.107	0.7t	0.150
	t > 0.107	0.7t	1.4t
Ultrasound	t > 0.100	0.030	0.300
		0.065	0.130

Acknowledgments

This work was funded by the New Mexico Space Grant. We would like to express thanks to Darin Franzoni (WSTF) for writing MATLAB code to properly import and apply filtering algorithms to scan data and to Buzz Wincheski (NASA-Langley Research Center) for guidance concerning scan settings and data post processing methods.

References

1. ASM International Handbook Committee, *ASM Handbook, Volume 17-Nondestructive Evaluation and Quality Control,* ASM International, 1989, pp. 164-194.

2. Russell A. Wincheski, *Eddy Current COPV Overwrap and Liner Thickness Measurement System and Data Analysis for 40-Inch Kevlar COPVs SN002 and SN027,* NASA/TM-2008-215105, Langley Research Center, Hampton, VA, Jan. 2008.

3. Buzz Wincheski, Jim Fulton, Shridhar Nath, and Min Namkung, *New Eddy Current Probe for Thickness Gauging of Conductive Materials*, NASA Langley Research Center, Hampton, VA, 1993.

4. J.B. Chang, *Implementation Guidelines for ANSI/AIAA S-081: Space Systems Composite Overwrapped Pressure Vessels,* The Aerospace Corporation, Vehicle Systems Division, El Segundo, CA, 2003.